

---

# Learning Ordinary Differential Equations with the Line Integral Loss Function

---

Anonymous Author(s)

Affiliation

Address

email

## Abstract

1 A new training method for learning representations of dynamical systems with  
2 neural networks is derived using a loss function based on line integrals from vec-  
3 tor calculus. The new training method is shown to learn the direction part of an  
4 ODE vector field with more accuracy and faster convergence compared to tradi-  
5 tional methods. The learned direction can then be combined with another model  
6 that learns the magnitude explicitly to decouple the learning process of an ODE  
7 into two separate easier problems. It can also be used as a feature generator for  
8 time-series classification problems, performing well on motion classification of  
9 dynamical systems. The new method does however have multiple limitations that  
10 overall make the method less generalizable and only suited for some specific type  
11 of problems.

## 12 1 Introduction

13 The theory of dynamical systems is widely applicable for modeling problems in fields like physics,  
14 engineering and medicine. This approach will often rely on creating explicit system models resulting  
15 in differential equations. But there are systems where creating explicit models are too difficult to  
16 realistically achieve for various reasons. This motivates the use of deep learning based methods to  
17 learn representations for dynamical systems.

18 The Neural ODE framework [1] [2] [3] defines a neural network architecture as the limit of a residual  
19 network, thus ending up with an ordinary differential equation. The forward pass is computed by  
20 numerically integrating the network ODE forwards in time, and the backward pass by integrating  
21 the adjoint system backwards in time. Because of the inherent ODE structure of Neural ODEs they  
22 are capable of learning dynamical systems by training on sampled trajectories.

23 This paper presents an alternative training method by utilizing a new loss function based on line  
24 integrals. The training method is slightly faster compared to adjoint based methods, while also  
25 generalizing better when learning ODEs. However, there are multiple limitations with the new  
26 training method which makes it overall less general. The loss function is derived in the next section.

## 27 2 The Line Integral Loss

### 28 2.1 Loss Function

29 Consider an autonomous ODEs on the form  $\dot{x} = f(x)$  with state vector  $x \in \mathbb{R}^m$  and system  
30 dynamics  $f : \mathbb{R}^m \rightarrow \mathbb{R}^m$ . Initial conditions  $x(t_0)$  will then evolve in time such that the trajectory  
31  $x(t)$  in the state space is tangent to the vector field  $f$ .

32 Now consider the case where the system dynamics  $f$  are unknown but with access to a dataset con-  
 33 sisting of  $n$  trajectories  $\mathbf{x}_1(t), \mathbf{x}_2(t), \dots, \mathbf{x}_n(t)$  where each trajectory is sampled from the system  
 34 at discrete points in time  $t_0, \dots, t_1$ . A method for training neural network representations of  $f$   
 35 can be derived by using the fact that trajectories are tangent to the underlying vector field. Define  
 36 a neural network on the form  $\dot{\mathbf{x}} = \mathbf{h}(\mathbf{x}; \boldsymbol{\theta})$  where  $\mathbf{h}(\mathbf{x}; \boldsymbol{\theta})$  is the represented as a neural network  
 37 parametrized by  $\boldsymbol{\theta}$ . The line integral of a vector field  $\mathbf{h}(\mathbf{x}; \boldsymbol{\theta})$  and trajectory  $\mathbf{x}_k(t)$  is defined as  
 38  $\int \mathbf{h} \cdot d\mathbf{x}_k = \int_{t_{k0}}^{t_{k1}} \mathbf{h}(\mathbf{x}_k(t); \boldsymbol{\theta})^T \mathbf{x}'_k(t) dt$  with  $\mathbf{x}'_k(t) = \frac{d\mathbf{x}_k(t)}{dt}$ .

39 A key observation is that the line integral takes its maximum value when the vector field and tra-  
 40 jectory perfectly align, and its minimum value when they are perfectly opposed. However, when  
 41 the vector field is represented by a neural network the line integral becomes potentially unbounded.  
 42 This can be solved by normalizing both vectors inside the integral to make their lengths equal to  
 43 1. Dividing by the length of the interval makes the total line integral bounded between 1 and  $-1$ .  
 44 Averaging over the trajectories in the training set then leads to the following optimization problem:

$$\min_{\boldsymbol{\theta}} \mathcal{L} = -\frac{1}{n} \sum_{k=1}^n \frac{1}{t_{k1} - t_{k0}} \int_{t_{k0}}^{t_{k1}} \frac{\mathbf{h}(\mathbf{x}_k(t); \boldsymbol{\theta})^T \mathbf{x}'_k(t)}{\|\mathbf{h}(\mathbf{x}_k(t); \boldsymbol{\theta})\| \|\mathbf{x}'_k(t)\|} dt \quad (1)$$

## 45 2.2 Gradients

46 Solving this unconstrained optimization problem can be done with any gradient based methods  
 47 commonly used in deep learning, but requires the gradient of the loss function to be known. The  
 48 gradients from the loss function to the parameters can be derived to the form:

$$\frac{\partial \mathcal{L}}{\partial \boldsymbol{\theta}} = -\frac{1}{n} \sum_{k=1}^n \frac{1}{t_{k1} - t_{k0}} \int_{t_{k0}}^{t_{k1}} \frac{\mathbf{x}'_k(t)}{\|\mathbf{x}'_k(t)\|}{}^T \left[ \frac{\mathbf{I}}{\|\mathbf{h}\|} - \frac{\mathbf{h}\mathbf{h}^T}{\|\mathbf{h}\|^3} \right] \frac{\partial \mathbf{h}}{\partial \boldsymbol{\theta}} dt \quad (2)$$

49 The vector-Jacobian product inside the integral can be computed efficiently using automatic dif-  
 50 ferentiation. It is also worth noting that if all the trajectories have the same start time  $t_0$  and end  
 51 time  $t_1$  it is possible to swap the order of the integral and the summation. This is often useful for  
 52 vectorization purposes, which can give a significant speedup.

53 The full gradient derivation is given in Appendix A.

## 54 2.3 Practicalities

55 A significant limitation of the normalization is that the magnitude of the vector field is lost when  
 56 training. In practice, the magnitude often goes towards 1 after training for enough epochs. The next  
 57 section demonstrates some experiments that use loss function even with this limitation.

58 Another drawback of the loss function is that it requires access to the time derivatives of the trajec-  
 59 tories in the dataset, unlike the standard Neural ODE approach which can learn dynamical system  
 60 representations without derivatives. However, this limitation can be overcome by approximating the  
 61 derivatives using a finite difference scheme if the sample interval  $h$  is small enough, and without too  
 62 noisy data:  $\frac{d\mathbf{x}_k(t_i)}{dt} \approx \frac{\mathbf{x}_k(t_{i+1}) - \mathbf{x}_k(t_i)}{h}$ .

63 Computing the integral numerically must also be done with consideration to the discretely sampled  
 64 trajectory points. A simple numerical method that works well enough is to use the trapezoid integra-  
 65 tion method, which can be implemented in an efficient way that does not require any more function  
 66 calls than a simple Riemann sum approximation. More advanced numerical integration methods  
 67 turns out in practice to be significantly more computationally expensive while only giving marginal  
 68 improvements to performance.

# 69 3 Experiments

## 70 3.1 Learning Dynamical Systems

71 A model is trained with the normalized line integral loss function and compared against other types  
 72 of models to determine how well the training method works. All the models are set up with the same

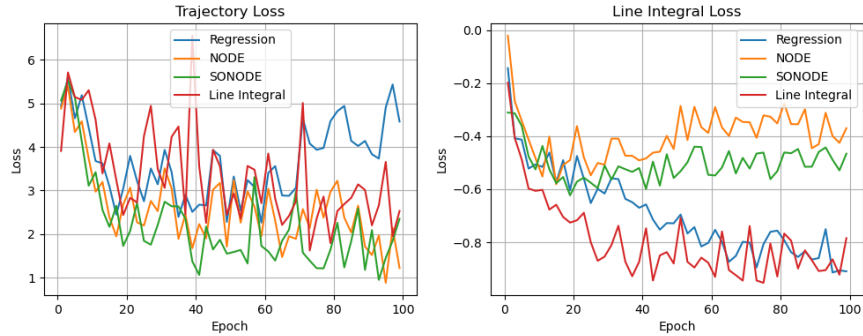


Figure 1: Loss values when training ODE models on a double pendulum system. Both loss functions are evaluated on the testing set.

73 underlying neural network structure. The models to compare against are: a basic regression model  
 74 that directly models the relation between a point  $\mathbf{x}(t)$  and its time derivative  $\dot{\mathbf{x}}(t)$ , a Neural ODE  
 75 (NODE) [1] that learns without knowing derivatives and finally a Second Order Neural ODE (SON-  
 76 ODE) [4]. The regression model uses the MSE loss function applied to predicted derivatives and  
 77 true derivatives when training, while the NODE models are trained by integrating numerically and  
 78 comparing points along the trajectory also using the MSE loss, followed by gradient computation  
 79 with the adjoint method.

80 The line integral model is set up to only learn the direction of the underlying vector field. Therefore  
 81 the line integral model is combined with a regression model similar to the one above that only learns  
 82 the magnitude. The final learned vector field is then the multiplication of the output of the two  
 83 models. Decoupling the vector field into direction and magnitude turns out to be an easier problem  
 84 to learn than directly regressing on the whole vector field.

85 The models are trained on the same trajectories sampled from a double pendulum system, which  
 86 is nonlinear and chaotic making the learning process non-trivial. The trajectories are generated  
 87 by integrating the system numerically. Normally distributed noise is also added to the training  
 88 points, and the noise is added before the derivatives are computed with finite differences to make the  
 89 setting more realistic. All the details regarding the experiment and implementation are described in  
 90 Appendix B.

91 To compare the models, two different loss functions are computed over a testing set each epoch. The  
 92 first is similar to the loss for the NODE models in that trajectories are integrated from initial values  
 93 and compared pointwise with the MSE loss function. The second is the normalized line integral  
 94 computed over the learned vector fields of the models.

95 Figure 1 shows the resulting test losses from training all the models on the double pendulum. Look-  
 96 ing at the trajectory loss it might seem that the basic regression model starts to overfit on the training  
 97 data, and thus falls behind the other models which are all approximately performing the same. When  
 98 looking at the line integral loss it is clear that the NODE and SONODE models perform significantly  
 99 worse than the regression and line integral models.

### 100 3.2 Motion Classification

101 Now consider a time-series classification problem where the goal is to classify trajectories sampled  
 102 from different dynamical systems. This experiment uses a double pendulum as the first system,  
 103 and a double pendulum being controlled by a PD-controller as the second system, making a binary  
 104 classification problem. A simple approach is to train a model consisting of an LSTM followed by  
 105 a classifier head. This classifier will be used as a baseline for comparison. The second classifier  
 106 will work by training two different line integral models on the two systems separately. To classify a  
 107 new trajectory, line integrals are computed for both models and used as features for another classifier  
 108 model. This experiment uses a Support Vector Classifier (SVC). More details are found in Appendix  
 109 B.

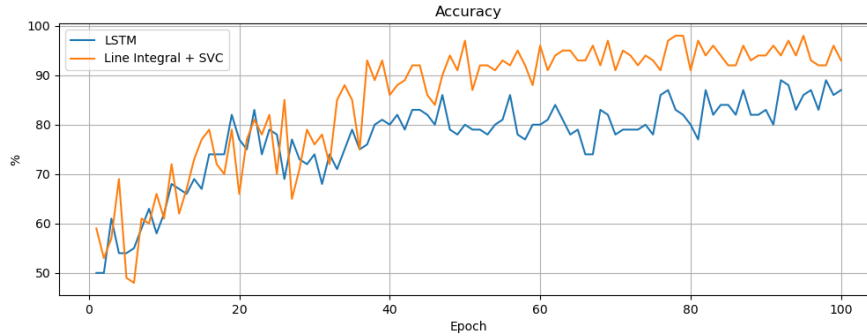


Figure 2: Classification accuracy from training two classifiers on time-series sampled from two different double pendulum systems. Evaluated on the testing set.

110 Figure 2 displays the classification accuracy on the testing set for each epoch when training the  
 111 classifiers described above. The SVC is reset and trained from scratch each epoch, to show how  
 112 the accuracy improves as the line integral models learn their vector fields. The line integral + SVC  
 113 classifier clearly outperforms the simple LSTM classifier.

#### 114 4 Discussion

115 When learning dynamical systems, the line integral model is comparable in loss values to the NODE  
 116 models, while significantly outperforming them on the line integral loss. This could be an indication  
 117 that the line integral model learns the overall structure of the vector field better, while the NODE  
 118 models are better at integrating trajectories that move initial points to their ending points without  
 119 considering the details of the structure. It does however also require an additional model to learn  
 120 the magnitude, which doubles the parameter count at the current setup. Other similar models could  
 121 also have been useful to benchmark against to get a better overview, such as the Hamiltonian [5] and  
 122 Lagrangian [6] Neural ODE models.

123 The line integral model is dependent on derivatives, so if the datasets were sampled at a lower  
 124 frequency or contained too much noise, the derivatives could easily become too inaccurate to make  
 125 the training reliable. Another consideration is that the training method only makes sense for learning  
 126 dynamical systems directly, while the NODE models are more general and comparable to residual  
 127 networks [7]. The gradients of the line integral loss is currently only defined to the parameters, and  
 128 finding gradients to the input does not necessarily make as much sense because the whole trajectory  
 129 must be considered as the input.

130 The motion classification experiment showcases how the line integral model can be used without  
 131 the magnitude. The LSTM model is not optimized well and could probably gain much better per-  
 132 formance. Other more advanced methods could also be used for comparison, but the main goal of  
 133 the experiment above is to show that it is possible to use the feature generation in this manner. The  
 134 current setup is also straightforward to extend to more than two classes.

135 The line integral method could also be extended to learning non-autonomous systems, meaning  
 136 systems that also depend on time explicitly. The network could be constructed to handle time, for  
 137 example taking inspiration from [8].

#### 138 5 Conclusion

139 This paper presents a new method for learning representations for dynamical systems that is derived  
 140 and experimentally tested. The method has some advantages over previous methods on certain  
 141 problems, but also has many limitations making the method less useful in the general case. Future  
 142 work could look into how to also learn the magnitude in a more efficient manner.

## References

- 143
- 144 [1] Ricky T. Q. Chen, Yulia Rubanova, Jesse Bettencourt, and David K Duvenaud. Neural ordinary  
145 differential equations. In S. Bengio, H. Wallach, H. Larochelle, K. Grauman, N. Cesa-Bianchi,  
146 and R. Garnett, editors, *Advances in Neural Information Processing Systems*, volume 31. Cur-  
147 ran Associates, Inc., 2018. URL [https://proceedings.neurips.cc/paper/2018/file/  
148 69386f6bb1dfed68692a24c8686939b9-Paper.pdf](https://proceedings.neurips.cc/paper/2018/file/69386f6bb1dfed68692a24c8686939b9-Paper.pdf).
- 149 [2] Emilien Dupont, Arnaud Doucet, and Yee Whye Teh. Augmented neural odes, 2019.
- 150 [3] Stefano Massaroli, Michael Poli, Jinkyoo Park, Atsushi Yamashita, and Hajime Asama. Dis-  
151 secting neural odes, 2021.
- 152 [4] Alexander Norcliffe, Cristian Bodnar, Ben Day, Nikola Simidjievski, and Pietro Liò. On sec-  
153 ond order behaviour in augmented neural odes, 2020. URL [https://arxiv.org/abs/2006.  
154 07220](https://arxiv.org/abs/2006.07220).
- 155 [5] Samuel Greydanus, Misko Dzamba, and Jason Yosinski. Hamiltonian neural net-  
156 works. In *Advances in Neural Information Processing Systems*, volume 32. Curran As-  
157 sociates, Inc., 2019. URL [https://proceedings.neurips.cc/paper/2019/file/  
158 26cd8ecadce0d4efd6cc8a8725cbd1f8-Paper.pdf](https://proceedings.neurips.cc/paper/2019/file/26cd8ecadce0d4efd6cc8a8725cbd1f8-Paper.pdf).
- 159 [6] Miles Cranmer, Sam Greydanus, Stephan Hoyer, Peter Battaglia, David Spergel, and Shirley  
160 Ho. Lagrangian neural networks, 2020. URL <https://arxiv.org/abs/2003.04630>.
- 161 [7] Kaiming He, Xiangyu Zhang, Shaoqing Ren, and Jian Sun. Deep residual learning for image  
162 recognition. In *2016 IEEE Conference on Computer Vision and Pattern Recognition (CVPR)*,  
163 pages 770–778, 2016. doi: 10.1109/CVPR.2016.90.
- 164 [8] Jared Quincy Davis, Krzysztof Choromanski, Jake Varley, Honglak Lee, Jean-Jacques E.  
165 Slotine, Valerii Likhosterov, Adrian Weller, Ameesh Makadia, and Vikas Sindhwani. Time  
166 dependence in non-autonomous neural odes. *CoRR*, abs/2005.01906, 2020. URL [https:  
167 //arxiv.org/abs/2005.01906](https://arxiv.org/abs/2005.01906).
- 168 [9] Kaare Brandt Petersen and Michael Syskind Pedersen. The matrix cookbook. 2008.
- 169 [10] Diederik P. Kingma and Jimmy Ba. Adam: A method for stochastic optimization, 2017.

# 170 Appendices

## 171 A Gradient Derivation

$$\begin{aligned}
\frac{\partial \mathcal{L}}{\partial \boldsymbol{\theta}} &= \frac{\partial}{\partial \boldsymbol{\theta}} \left[ -\frac{1}{n} \sum_{k=1}^n \frac{1}{t_{k_1} - t_{k_0}} \int_{t_{k_0}}^{t_{k_1}} \frac{\mathbf{h}(\mathbf{x}_k(t); \boldsymbol{\theta})}{\|\mathbf{h}(\mathbf{x}_k(t); \boldsymbol{\theta})\|} \frac{\mathbf{x}'_k(t)}{\|\mathbf{x}'_k(t)\|} dt \right] \\
&= -\frac{1}{n} \sum_{k=1}^n \frac{1}{t_{k_1} - t_{k_0}} \int_{t_{k_0}}^{t_{k_1}} \frac{\partial}{\partial \boldsymbol{\theta}} \left[ \frac{\mathbf{h}(\mathbf{x}_k(t); \boldsymbol{\theta})}{\|\mathbf{h}(\mathbf{x}_k(t); \boldsymbol{\theta})\|} \frac{\mathbf{x}'_k(t)}{\|\mathbf{x}'_k(t)\|} \right] dt \\
&= -\frac{1}{n} \sum_{k=1}^n \frac{1}{t_{k_1} - t_{k_0}} \int_{t_{k_0}}^{t_{k_1}} \frac{\mathbf{x}'_k(t)}{\|\mathbf{x}'_k(t)\|} \frac{\partial}{\partial \boldsymbol{\theta}} \left[ \frac{\mathbf{h}(\mathbf{x}_k(t); \boldsymbol{\theta})}{\|\mathbf{h}(\mathbf{x}_k(t); \boldsymbol{\theta})\|} \right] dt
\end{aligned} \tag{3}$$

172 The partial derivative  $\frac{\partial}{\partial \boldsymbol{\theta}} \left[ \frac{\mathbf{h}(\mathbf{x}_k(t); \boldsymbol{\theta})}{\|\mathbf{h}(\mathbf{x}_k(t); \boldsymbol{\theta})\|} \right] = \frac{\partial}{\partial \boldsymbol{\theta}} \frac{\mathbf{h}}{\|\mathbf{h}\|}$  can then be expanded using the chain rule:

$$\frac{\partial}{\partial \boldsymbol{\theta}} \frac{\mathbf{h}}{\|\mathbf{h}\|} = \left[ \frac{\partial}{\partial \mathbf{h}} \frac{\mathbf{h}}{\|\mathbf{h}\|} \right] \frac{\partial \mathbf{h}}{\partial \boldsymbol{\theta}} \tag{4}$$

173 The innermost partial derivative  $\frac{\partial}{\partial \mathbf{h}} \frac{\mathbf{h}}{\|\mathbf{h}\|}$  can be computed explicitly using the following formula for  
174 differentiating a normalized vector [9]:

$$\frac{\partial}{\partial \mathbf{x}} \frac{\mathbf{x} - \mathbf{a}}{\|\mathbf{x} - \mathbf{a}\|} = \frac{\mathbf{I}}{\|\mathbf{x} - \mathbf{a}\|} - \frac{(\mathbf{x} - \mathbf{a})(\mathbf{x} - \mathbf{a})^T}{\|\mathbf{x} - \mathbf{a}\|^3} \tag{5}$$

175 with  $\mathbf{x} = \mathbf{h}$  and  $\mathbf{a} = \mathbf{0}$ . This leads to the expression for the gradient of the normalized vector as:

$$\frac{\partial}{\partial \boldsymbol{\theta}} \frac{\mathbf{h}}{\|\mathbf{h}\|} = \left[ \frac{\mathbf{I}}{\|\mathbf{h}\|} - \frac{\mathbf{h}\mathbf{h}^T}{\|\mathbf{h}\|^3} \right] \frac{\partial \mathbf{h}}{\partial \boldsymbol{\theta}}$$

176 Inserting this into equation (3) leads to the final gradient expression:

$$\frac{\partial \mathcal{L}}{\partial \boldsymbol{\theta}} = -\frac{1}{n} \sum_{k=1}^n \frac{1}{t_{k_1} - t_{k_0}} \int_{t_{k_0}}^{t_{k_1}} \frac{\mathbf{x}'_k(t)}{\|\mathbf{x}'_k(t)\|} \left[ \frac{\mathbf{I}}{\|\mathbf{h}\|} - \frac{\mathbf{h}\mathbf{h}^T}{\|\mathbf{h}\|^3} \right] \frac{\partial \mathbf{h}}{\partial \boldsymbol{\theta}} dt \tag{6}$$

177 Additionally, if all the sample times are the same  $t_0, \dots, t_1$ , the order of the sum and integration can  
178 be swapped:

$$\frac{\partial \mathcal{L}}{\partial \boldsymbol{\theta}} = -\frac{1}{n} \frac{1}{t_1 - t_0} \int_{t_0}^{t_1} \sum_{k=1}^n \frac{\mathbf{x}'_k(t)}{\|\mathbf{x}'_k(t)\|} \left[ \frac{\mathbf{I}}{\|\mathbf{h}\|} - \frac{\mathbf{h}\mathbf{h}^T}{\|\mathbf{h}\|^3} \right] \frac{\partial \mathbf{h}}{\partial \boldsymbol{\theta}} dt \tag{7}$$

## 179 B Experimental Details

### 180 B.1 Implementation

181 A PyTorch implementation of both experiments be found at this [anonymous repository](#).

### 182 B.2 Data Generation

183 The controlled double pendulum system can be written as an ODE on the state-space form:

$$\frac{d}{dt} \begin{bmatrix} q_1 \\ q_2 \\ \dot{q}_1 \\ \dot{q}_2 \end{bmatrix} = \begin{bmatrix} \dot{q}_1 \\ \dot{q}_2 \\ (m_1 + m_2)l_1^2 & m_2l_1l_2 \cos(q_1 - q_2) \\ m_2l_1l_2 \cos(q_1 - q_2) & m_2l_2^2 \end{bmatrix}^{-1} \begin{bmatrix} -m_2l_1l_2 \sin(q_1 - q_2)\dot{q}_2^2 - (m_1 + m_2)gl_1 \sin q_1 + u_1 \\ m_2l_1l_2 \sin(q_1 - q_2)\dot{q}_1^2 - m_2gl_2 \sin q_2 + u_2 \end{bmatrix} \quad (8)$$

184 with a four dimensional state vector  $[q_1 \ q_2 \ \dot{q}_1 \ \dot{q}_2]^T$  and two dimensional input vector  
185  $[u_1 \ u_2]^T$ . All experiments uses the parameters  $m_1 = 1, m_2 = 1, l_1 = 1, l_2 = 1, g = 9.81$   
186 for simplicity.

187 A new batch of size 200 is generated for every epoch during training by integrating the double  
188 pendulum (8) using a step size of  $h = 0.01$  from  $t_0 = 0$  to  $t_1 = 1$ . The initial values to be  
189 integrated are randomly sampled uniformly in a box around the origin. A testing batch of size 20  
190 is also generated at every epoch to evaluate the performance on the two loss functions in Figure 1.  
191 Normally distributed noise with mean 0 and standard deviation 0.01 is added to the training batch,  
192 and then derivatives are computed with finite differences after the noise is added.

193 All the experiments are ran with the same seeding so that the data generation remains the same.

### 194 B.3 Learning Dynamical Systems

195 The input is set to  $u_1 = u_2 = 0$ .

196 All the trained models use the same neural network structure consisting of 6 linear layers with the  
197 tanh activation function in between layers. The layers has nodes: 4, 50, 100, 200, 100, 50, 4, except  
198 for the SONODE with 2 output nodes and the magnitude regression part of the line integral model  
199 with 1 output node. All the models are trained with the Adam optimizer [10] using a learning rate  
200 of 0.001.

201 The line integral model is combined with the magnitude regression model by first normalizing the  
202 output of the line integral model and then multiplying with the magnitude. The line integral usually  
203 converges to a magnitude of 1 after some time, but the normalization makes it more stable when  
204 evaluating on the testing set early.

205 When training the line integral model it is not actually necessary to compute the line integral, only  
206 the gradients (2) are necessary. But the line integral can still be useful to compute to determine if  
207 the loss is decreasing.

208 Finally, the two loss functions evaluated on the testing set are the trajectory loss and the line integral  
209 loss. The trajectory loss takes the first values of the test batch and integrates these as intial values on  
210 the trained model. During integration, points are sampled at the same points in time as the testing  
211 batch. The integrated trajectories are then compared to the full testing trajectories using the MSE  
212 loss. The line integral loss function is computed by using the derivatives of the testing trajectories  
213 with the trained models. The derivatives of the testing batch are also approximated using finite  
214 differences, but without any noise.

### 215 B.4 Motion Classification

216 Two systems are now used for data generation: one uncontrolled double pendulum similar to the  
217 previous experiment and one controlled with a PD-controller. The controller is on the form:  $u_1 =$   
218  $-0.1q_1 - 0.01\dot{q}_1$  and  $u_2 = -5(q_2 - q_1) - 2\dot{q}_2$ . This ends up driving the second joint angle towards the

219 same angle as the first joint, while also slowing down the overall system. This causes the pendulum  
220 to appear more constrained in its motion.

221 The LSTM classifier consists of an LSTM layer with 300 hidden units followed by a neural network  
222 with layers of nodes: 300, 150, 1 and sigmoid activations in between. It is trained as a binary clas-  
223 sification problem on trajectories from the two systems using the Adam optimizer using a learning  
224 rate of 0.001 and the binary cross entropy loss function.

225 The second model trains two line integral models separately on the two double pendulum systems.  
226 These models are used as feature generators by computing normalized line integrals with trajectories  
227 to see how well they align with the two vector fields. These alignments can then be used to classify  
228 them. The simplest classifier would be to simply see what double pendulum system the trajectory  
229 aligns the most with. However, as the two systems can produce similar looking trajectories, this  
230 approach will not always be perfect. So for each trajectory to be classified, the line integral of both  
231 models are used as features for a new classifier model, here using an SVC. Figure 2 shows accuracy  
232 over time by re-training the SVC from scratch each epoch, but the simplest approach would be to  
233 fully train the two line integral models first, and then train the classifier afterwards.